Monte Carlo simulation of single spin asymmetries in pion-proton collisions

Andrea Bianconi*

*Dipartimento di Chimica e Fisica per l'Ingegneria e per i Materiali, Università di Brescia, I-25123 Brescia, Italy,
and Istituto Nazionale di Fisica Nucleare, Sezione di Pavia, I-27100 Pavia, Italy*

Marco Radici†

*Dipartimento di Fisica Nucleare e Teorica, Università di Pavia,
and Istituto Nazionale di Fisica Nucleare, Sezione di Pavia, I-27100 Pavia, Italy*

We present Monte Carlo simulations of both the Sivers and the Boer-Mulders effects in the polarized Drell-Yan $\pi^{\pm} p^{\uparrow} \rightarrow \mu^+ \mu^- X$ process at a kinematics suitable to the COMPASS setup. For the Sivers effect, we adopt two different parametrizations for the Sivers function to explore the statistical accuracy required to extract unambiguous information on this parton density. In particular, we verify the possibility of checking its predicted sign change between semi-inclusive deep-inelastic scattering (SIDIS) and Drell-Yan processes, a crucial test of nonperturbative QCD. For the Boer-Mulders effect, because of the lack of parametrizations we can make only guesses. The goal is to explore the possibility of extracting information on the transversity distribution, the missing piece necessary to complete the knowledge of the nucleon spin structure at leading twist, and the Boer-Mulders function, which is related to the long-standing problem of the violation of the Lam-Tung sum rule in the unpolarized Drell-Yan cross section.

I. INTRODUCTION

The recent measurement of single-spin asymmetries (SSA) in semi-inclusive $lp^{\uparrow} \rightarrow l' \pi X$ deep-inelastic scattering (SIDIS) on transversely polarized hadronic targets [1–4] has renewed the interest in the problem of describing the spin structure of hadrons within quantum chromodynamics (QCD) [5], and has stimulated since then a large production of phenomenological and theoretical papers. Experimental evidence of large SSA in hadron-hadron collisions was well known for many years [6,7], but it has never been consistently explained in the context of perturbative QCD in the collinear massless approximation [8]. The idea of going beyond the collinear approximation opened new perspectives about the possibility of explaining these SSA in terms of intrinsic transverse motion of partons inside hadrons, and of correlations between such intrinsic transverse momenta and transverse spin degrees of freedom. The most popular examples are the Sivers [9] and the Collins [10] effects. In the former case, an asymmetric azimuthal distribution of detected hadrons (with respect to the normal to the production plane) is obtained from the nonperturbative correlation $\boldsymbol{p}_T \times \boldsymbol{P} \cdot \boldsymbol{S}_T$, where $\boldsymbol{p}_T$ is the intrinsic transverse momentum of an unpolarized parton inside a target hadron with momentum $\boldsymbol{P}$ and transverse polarization $\boldsymbol{S}_T$. In the latter case, the asymmetry is obtained from the correlation $\boldsymbol{k} \times \boldsymbol{P}_{hT} \cdot \boldsymbol{s}_T$, where a parton with momentum $\boldsymbol{k}$ and transverse polarization $\boldsymbol{s}_T$ fragments into an unpolarized hadron with transverse momentum $\boldsymbol{P}_{hT}$. In both cases, the sizes of the effects are

represented by new transverse-momentum dependent (TMD) partonic functions, the so-called Sivers and Collins functions, respectively.

However, SSA data in hadronic collisions have been collected so far typically for semi-inclusive $pp^{(\uparrow)} \rightarrow h^{(\uparrow)} X$ processes, where the factorization proof is complicated by higher-twist correlators [11] and the power-suppressed asymmetry can be produced by several (overlapping) mechanisms. On the contrary, the theoretical situation of the SIDIS measurements is more transparent. On the basis of a suitable factorization theorem [12,13], the cross section at leading twist contains convolutions involving separately the Sivers and Collins functions with different azimuthal dependences, $\sin(\phi - \phi_S)$ and $\sin(\phi + \phi_S)$, respectively, where ϕ, ϕ_S, are the azimuthal angles of the produced hadron and of the target polarization with respect to the axis defined by the virtual photon [14]. According to the extracted azimuthal dependence, the measured SSA can then be clearly related to one effect or the other [1,2].

Similarly, in the Drell-Yan process $H_1 H_2^{\uparrow} \rightarrow l^+ l^- X$ the cross section displays at leading twist two terms weighted by $\sin(\phi - \phi_S)$ and $\sin(\phi + \phi_S)$, where now ϕ, ϕ_S, are the azimuthal orientations of the final lepton plane and of the hadron polarization with respect to the reaction plane [15]. Adopting the notations recommended in Ref. [16], the first one involves the convolution of the Sivers function $f_{1T}^{\perp}$ with the standard unpolarized parton distribution f_1. The second one involves the transversity distribution h_1 and the Boer-Mulders function $h_1^{\perp}$, a TMD distribution which is most likely responsible for the violation of the Lam-Tung sum rule in the corresponding anomalous $\cos 2\phi$ asymmetry of the unpolarized Drell-Yan cross sec-

─────────
*Electronic address: andrea.bianconi@bs.infn.it
†Electronic address: marco.radici@pv.infn.it

tion [15]. Hence, a simultaneous measurement of unpolarized and single-polarized Drell-Yan cross sections would allow one to extract all the unknowns from data [17,18]. Both h_1 and $h_1^\perp$ describe the distribution of transversely polarized partons; but the former applies to transversely polarized parent hadrons, while the latter to unpolarized ones. On an equal footing, $f_{1T}^\perp$ and f_1 describe distributions of unpolarized partons. The correlation between $\boldsymbol{p}_T$ and $\boldsymbol{S}_T$ inside $f_{1T}^\perp$ is possible only for a nonvanishing orbital angular momentum of partons. Then, extraction of Sivers function from SIDIS and Drell-Yan data would allow one to study the orbital motion and the spatial distribution of hidden confined partons [19], as well as to test its peculiar universality property [20].

In a series of previous papers, we performed numerical simulations of single-polarized Drell-Yan SSA for the $pp^\uparrow \to \mu^+\mu^- X$ [21] and $\bar{p}p^\uparrow \to \mu^+\mu^- X$ [17] processes. With proton beams, we considered collisions at $\sqrt{s} = 200$ GeV in the kinematic conditions for the foreseen upgrade of RHIC (RHIC II). Even if in pp collisions the nonvalence partonic contribution to the elementary annihilation is unavoidable (leading, in principle, to lower counting rates), still the kinematics selects a portion of phase space that emphasizes this contribution. The net result is that with a reasonable sample of Drell-Yan events the statistical accuracy allows one to unambiguously extract the Sivers function from the corresponding $\sin(\phi - \phi_S)$ asymmetry, as well as to clearly test its predicted sign change with respect to the SIDIS asymmetry [21]. In $\bar{p}p$ collisions, the cross section is dominated by the valence contribution to the annihilation of a parton (from p) and an antiparton (from $\bar{p}$); hence, in general, it is not suppressed as in the previous case (for a quantitative check in our Monte Carlo, see Sec. IV B of Ref. [21]). In Ref. [17], we selected antiproton beams of 15 GeV, as they could be produced at the high energy storage ring (HESR) at GSI [22,23], and we simulated collisions at $\sqrt{s} \sim 14$ GeV in the so-called asymmetric collider mode. The goal was to explore the minimal conditions required for an unambiguous extraction of h_1 and $h_1^\perp$ from a combined analysis of the $\sin(\phi + \phi_S)$ and $\cos 2\phi$ asymmetries in the full (unpolarized + polarized) cross section.

Here, we will reconsider the same scenarios but for the $\pi^\pm p^\uparrow \to \mu^+\mu^- X$ process using the pion beam at COMPASS. As for $\bar{p}$ beams, the elementary mechanism is dominated by the annihilation between valence partons (from p) and valence antipartons (from π). Indeed, a large Sivers effect was predicted in this context by using the same Sivers function fitted to the measured $\sin(\phi - \phi_S)$ asymmetry in SIDIS [24]. Taking advantage on the high statistics reachable with pions, in our Monte Carlo we simulate both $\sin(\phi \pm \phi_S)$ SSA in the Drell-Yan cross section. For the Sivers effect we use two parametrizations of $f_{1T}^\perp$: the one of Ref. [25], which was deduced by fitting the recent HERMES data for the $\sin(\phi - \phi_S)$ SSA [2]; the

one of Ref. [21], which is constrained by the recent RHIC data for the $pp^\uparrow \to \pi X$ process at higher energy [26]. For the Boer-Mulders effect, since there is no such abundance of data and fits, we follow Ref. [15] to constrain $h_1^\perp$ by the azimuthal asymmetry of the corresponding unpolarized Drell-Yan cross section (see also Refs. [27,28] for a similar analysis). Then, we insert, as we did in Ref. [17], very different input test functions for h_1 in order to explore the sensitivity of the simulated SSA within the statistical accuracy.

In Sec. II, we review the formalism and the details of the numerical simulation. In Sec. III, we present and discuss our results. Finally, in Sec. IV we draw some conclusions.

II. GENERAL FRAMEWORK FOR THE NUMERICAL SIMULATION

In a Drell-Yan process, an antilepton-lepton pair with individual momenta k_1 and k_2 is produced from the collision of two hadrons with momentum P_i, mass M_i, and spin S_i, with $i = 1, 2$. The center-of-mass (c.m.) square energy available is $s = (P_1 + P_2)^2$ and the invariant mass of the final lepton pair is given by the timelike momentum transfer $q^2 \equiv M^2 = (k_1 + k_2)^2$. If $M^2, s \to \infty$, while keeping the ratio $0 \le \tau = M^2/s \le 1$ limited, a factorization theorem can be proven [29] ensuring that the elementary mechanism proceeds through the annihilation of a parton and an antiparton with momenta p_1 and p_2, respectively, into a virtual photon with timelike momentum q^2. If P_1^+ and P_2^- are the dominant light-cone components of hadron momenta in this regime, then the partons are approximately collinear with the parent hadrons and carry the light-cone momentum fractions $0 \le x_1 = p_1^+/P_1^+$, $x_2 = p_2^-/P_2^- \le 1$, with $q^+ = p_1^+$, $q^- = p_2^-$ by momentum conservation [15]. The transverse components $\boldsymbol{p}_{iT}$ of p_i with respect to the direction defined by $\boldsymbol{P}_i (i = 1, 2)$, are constrained again by the momentum conservation $\boldsymbol{q}_T = \boldsymbol{p}_{1T} + \boldsymbol{p}_{2T}$, where $\boldsymbol{q}_T$ is the transverse momentum of the final lepton pair. If $\boldsymbol{q}_T \neq 0$ the annihilation direction is not known. Hence, it is convenient to select the so-called Collins-Soper frame [30] described in Fig. 1. The final lepton pair is detected in the solid angle (θ, ϕ), where, in particular, ϕ (and all other azimuthal angles) is measured
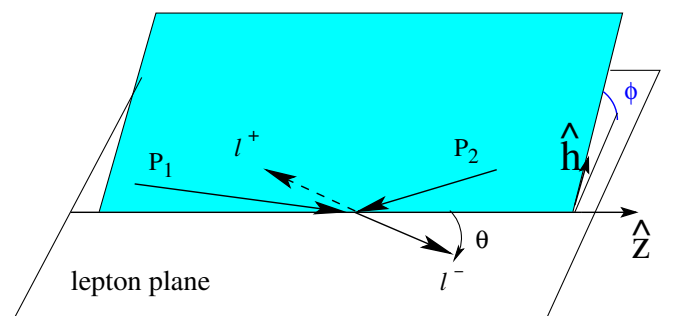

FIG. 1 (color online).   The Collins-Soper frame.

in a plane perpendicular to the indicated lepton plane but containing $\hat{\boldsymbol{h}} = \boldsymbol{q}_T/|\boldsymbol{q}_T|$.

The full expression of the leading-twist differential cross section for the $H_1 H_2^{\uparrow} \to l^+ l^- X$ process can be written as [15]

$$
\begin{aligned}
\frac{d\sigma}{d\Omega dx_1 dx_2 d\boldsymbol{q}_T} &= \frac{d\sigma^o}{d\Omega dx_1 dx_2 d\boldsymbol{q}_T} + \frac{d\Delta\sigma^{\uparrow}}{d\Omega dx_1 dx_2 d\boldsymbol{q}_T} \\
&= \frac{\alpha^2}{3Q^2}\sum_q e_q^2 \Bigg\{ A(y)\mathcal{F}[f_1^q(H_1)f_1^q(H_2)] + B(y)\cos 2\phi\, \mathcal{F}\Bigg[(2\hat{\boldsymbol{h}}\cdot\boldsymbol{p}_{1T}\hat{\boldsymbol{h}}\cdot\boldsymbol{p}_{2T} - \boldsymbol{p}_{1T}\cdot\boldsymbol{p}_{2T})\frac{h_1^{\perp q}(H_1)h_1^{\perp q}(H_2)}{M_1 M_2}\Bigg] \Bigg\} \\
&\quad + \frac{\alpha^2}{3Q^2}|\boldsymbol{S}_{2T}|\sum_q e_q^2 \Bigg\{ A(y)\sin(\phi-\phi_{S_2})\mathcal{F}\Bigg[\hat{\boldsymbol{h}}\cdot\boldsymbol{p}_{2T}\frac{f_1^q(H_1)f_{1T}^{\perp q}(H_2^{\uparrow})}{M_2}\Bigg] \\
&\quad - B(y)\sin(\phi+\phi_{S_2})\mathcal{F}\Bigg[\hat{\boldsymbol{h}}\cdot\boldsymbol{p}_{1T}\frac{h_1^{\perp q}(H_1)h_1^q(H_2^{\uparrow})}{M_1}\Bigg] \\
&\quad - B(y)\sin(3\phi-\phi_{S_2})\mathcal{F}\Bigg[(4\hat{\boldsymbol{h}}\cdot\boldsymbol{p}_{1T}(\hat{\boldsymbol{h}}\cdot\boldsymbol{p}_{2T})^2 - 2\hat{\boldsymbol{h}}\cdot\boldsymbol{p}_{2T}\boldsymbol{p}_{1T}\cdot\boldsymbol{p}_{2T} - \hat{\boldsymbol{h}}\cdot\boldsymbol{p}_{1T}p_{2T}^2)\frac{h_1^{\perp q}(H_1)h_{1T}^{\perp q}(H_2^{\uparrow})}{2M_1 M_2^2}\Bigg] \Bigg\},
\end{aligned}
$$

$$(1)$$

where α is the fine structure constant, $d\Omega = \sin\theta d\theta d\phi$, e_q is the charge of the parton with flavor q, ϕ_{S_i} is the azimuthal angle of the transverse spin of hadron i, and

$$
\begin{aligned}
A(y) &= (\tfrac{1}{2} - y + y^2) \stackrel{cm}{=} \tfrac{1}{4}(1 + \cos^2\theta) \\
B(y) &= y(1 - y) \stackrel{cm}{=} \tfrac{1}{4}\sin^2\theta.
\end{aligned}
\tag{2}
$$

The TMD functions $f_1^q(H)$, $h_1^{\perp q}(H)$, describe the distributions of unpolarized and transversely polarized partons in an unpolarized hadron H, respectively, while $f_{1T}^{\perp q}(H^{\uparrow})$ and the pair $h_1^q(H^{\uparrow})$, $h_{1T}^{\perp q}(H^{\uparrow})$, have a similar interpretation but for transversely polarized hadrons $H^{\uparrow}$. The convolutions are defined as

$$
\begin{aligned}
\mathcal{F}[DF_1^q(H_1)DF_2^q(H_2^{(\uparrow)})] &\equiv \int d\boldsymbol{p}_{1T}d\boldsymbol{p}_{2T}\delta(\boldsymbol{p}_{1T} + \boldsymbol{p}_{2T} - \boldsymbol{q}_T) \\
&\quad \times [DF_1(x_1, \boldsymbol{p}_{1T}; \bar{q}/H_1) \\
&\quad \times DF_2(x_2, \boldsymbol{p}_{2T}; q/H_2^{(\uparrow)}) \\
&\quad + (q \leftrightarrow \bar{q})].
\end{aligned}
\tag{3}
$$

In previous papers, we made numerical simulations of the SSA generated in Eq. (1) by the azimuthal dependences $\cos 2\phi$ and $\sin(\phi + \phi_{S_2})$ for antiproton beams $H_1 = \bar{p}$ [17], by the $\sin(\phi - \phi_{S_2})$ dependence for proton beams $H_1 = p$ [21], as well as for double-polarized Drell-Yan processes with $H_1^{\uparrow} = H_2^{\uparrow} = p^{\uparrow}$ [31]. A combined measurement of these SSA allows one to completely determine the intertwined unknown transversity h_1 and Boer-Mulders function $h_1^{\perp}$, and the Sivers function $f_{1T}^{\perp}$. The Monte Carlo simulation was performed for high-energy proton beams ($\sqrt{s} = 200$ GeV) in the conditions of the foreseen upgrade of RHIC (RHIC II), and for antiproton beams of 15 GeV as they could be produced at HESR-GSI. In the latter case, several scenarios were explored for $5 \lesssim$

$\sqrt{s} \lesssim 14$ GeV and $1.5 < M < 2.5$, $4 < M < 9$ GeV, in order to avoid overlaps with the strange, charm, and bottom quarkonia [where the elementary annihilation does not necessarily proceed through a simple intermediate virtual photon, as it is assumed in Eq. (1)]. Here, we reconsider the $\sin(\phi - \phi_{S_2})$ and $\sin(\phi + \phi_{S_2})$ asymmetries by using pion beams of 50–100 GeV as they can be produced at COMPASS, in the fixed target mode such as to approximately reach the same c.m. energy considered at HESR-GSI, namely $\sqrt{s} \sim 10$–14 GeV. Most of the technical details of the simulation are mutuated from our previous works; hence, we will heavily refer to Refs. [17,21] in the following.

The Monte Carlo events have been generated by the following cross section [17]:

$$
\frac{d\sigma}{d\Omega dx_1 dx_2 d\boldsymbol{q}_T} = K\frac{1}{s}|\mathcal{T}(\boldsymbol{q}_T, x_1, x_2, M)|^2 \sum_{i=1}^{4} c_i(\boldsymbol{q}_T, x_1, x_2) \times S_i(\theta, \phi, \phi_{S_2}),
\tag{4}
$$

where the event distribution is driven by the elementary unpolarized annihilation, whose transition amplitude $\mathcal{T}$ has been highlighted. In Eq. (1), we assume a factorized transverse-momentum dependence in each parton distribution such as to break the convolution $\mathcal{F}$, leading to

$$
|\mathcal{T}|^2 \approx A(q_T, x_1, x_2, M)F(x_1, x_2),
\tag{5}
$$

where $q_T \equiv |\boldsymbol{q}_T|$. The function A is parametrized and normalized as in Ref. [32], where high-energy Drell-Yan $\pi - p$ collisions were considered. The average transverse momentum turns out to be $\langle q_T \rangle > 1$ GeV/c (see also the more recent Ref. [33]), which effectively reproduces the influence of sizable QCD corrections beyond the parton model picture of Eq. (1). It is well known [34] that such corrections induce also large K factors and an M scale

dependence in parton distributions, determining their evolution. As in our previous works [17,21,31], we conventionally assume in Eq. (4) that $K = 2.5$, but we stress that in an azimuthal asymmetry the corrections to the cross sections in the numerator and in the denominator should compensate each other, as it turns out to actually happen at RHIC c.m. square energies [35]. Since the range of M values here explored is close to the one of Ref. [32], where the parametrization of A, F, and c_i in Eq. (4) was deduced assuming M-independent parton distributions, we keep our same previous approach [17,21,31] and use

$$F(x_1, x_2) = \frac{\alpha^2}{12Q^2} \sum_q e_q^2 f_1^q(x_1; \bar{q}/H_1) f_1^q(x_2; q/H_2) + (\bar{q} \leftrightarrow q),$$
(6)

where the unpolarized distribution $f_1^q(x)$ for various flavors $q = u$, d, s, is taken again from Ref. [32].

The whole solid angle (θ, ϕ) of the final lepton pair in the Collins-Soper frame is randomly distributed in each variable. The explicit form for sorting it in the Monte Carlo is [17,21]

$$\sum_{i=1}^4 c_i(q_T, x_1, x_2) S_i(\theta, \phi, \phi_{S_2}) = 1 + \cos^2\theta + \frac{\nu(x_1, x_2, q_T)}{2}$$
$$\times \sin^2\theta \cos 2\phi$$
$$+ |\mathbf{S}_{2T}| c_4(q_T, x_1, x_2)$$
$$\times S_4(\theta, \phi, \phi_{S_2}).$$
(7)

If quarks were massless, the virtual photon would be only transversely polarized and the angular dependence would be described by the functions $c_1 = S_1 = 1$ and $c_2 = 1$, $S_2 = \cos^2\theta$. Violations of such azimuthal symmetry induced by the function $c_3 \equiv \frac{\nu}{2}$ are due to the longitudinal polarization of the virtual photon and to the fact that quarks have an intrinsic transverse-momentum distribution, leading to the explicit violation of the so-called Lam-Tung sum rule [32]. QCD corrections influence ν, which in principle depends also on M^2 [32]. Azimuthal $\cos 2\phi$ asymmetries induced by ν were simulated in Ref. [17] using the simple parametrization of Ref. [15] and testing it against the previous measurement of Ref. [32].

If we consider the Sivers effect in Eq. (1), the last term in Eq. (7) becomes

$$S_4(\theta, \phi, \phi_{S_2}) = (1 + \cos^2\theta) \sin(\phi - \phi_{S_2})$$
(8)

and the corresponding coefficient c_4 reads

$$c_4(q_T, x_1, x_2) = \frac{\sum_q e_q^2 \mathcal{F}[\hat{\mathbf{h}} \cdot \mathbf{p}_{2T} \frac{f_1^q(x_1, \mathbf{p}_{1T}) f_{1T}^{\perp q}(x_2, \mathbf{p}_{2T})}{M_2}]}{\sum_q e_q^2 \mathcal{F}[f_1^q(x_1, \mathbf{p}_{1T}) f_1^q(x_2, \mathbf{p}_{2T})]},$$
(9)

where the complete dependence of the involved TMD parton distributions has been made explicit.

Vice versa, if we consider the Boer-Mulders effect in Eq. (1), the last term in Eq. (7) becomes

$$S_4(\theta, \phi, \phi_{S_2}) = \sin^2\theta \sin(\phi + \phi_{S_2})$$
(10)

and the corresponding coefficient c_4 reads

$$c_4(q_T, x_1, x_2) = -\frac{\sum_q e_q^2 \mathcal{F}[\hat{\mathbf{h}} \cdot \mathbf{p}_{1T} \frac{h_1^{\perp q}(x_1, \mathbf{p}_{1T}) h_1^q(x_2, \mathbf{p}_{2T})}{M_1}]}{\sum_q e_q^2 \mathcal{F}[f_1^q(x_1, \mathbf{p}_{1T}) f_1^q(x_2, \mathbf{p}_{2T})]}.$$
(11)

In the following, we will discuss different inputs for the x and $\mathbf{p}_T$ dependence of these distributions which allow one to calculate the convolutions and determine c_4. In any case, following Refs. [17,21,31], the general strategy is to divide the event sample in two groups, one for positive values "U" of S_4 in Eq. (8) or (10), and another one for negative values "D," then taking the ratio $(U - D)/(U + D)$. Data are accumulated only in the x_2 bin, i.e. they are summed upon x_1, θ, and q_T. Statistical errors for the spin asymmetry $(U - D)/(U + D)$ are obtained by making 10 independent repetitions of the simulation for each individual case, and then calculating for each x_2 bin the average asymmetry value and the variance. We checked that 10 repetitions are a reasonable threshold to have stable numbers, since the results do not change significantly when increasing the number of repetitions beyond 6.

A. The Sivers effect

Recently, the HERMES collaboration released new SSA data for the SIDIS process on transversely polarized protons [2], which substantially increase the precision of the previous data set [1]. As a consequence, different parametrizations of the Sivers function $f_{1T}^{\perp}$ have been extracted from this data set and found compatible also with the recent COMPASS data [4] (for a useful comparison among the various approaches see Ref. [36]). Following Ref. [21], we first simulate the Sivers effect using the parametrization of Ref. [25],

$$f_{1T}^{\perp q}(x, \mathbf{p}_T) = -2N_q \frac{(a_q + b_q)^{a_q + b_q}}{a_q^{a_q} b_q^{b_q}} x^{a_q} (1 - x)^{b_q}$$
$$\times \frac{M_2 M_0}{\mathbf{p}_T^2 + M_0^2} f_1^q(x, \mathbf{p}_T)$$
$$= -2N_q \frac{1}{\pi \langle p_T^2 \rangle} \frac{(a_q + b_q)^{a_q + b_q}}{a_q^{a_q} b_q^{b_q}} x^{a_q} (1 - x)^{b_q}$$
$$\times \frac{M_2 M_0}{\mathbf{p}_T^2 + M_0^2} e^{-p_T^2/\langle p_T^2 \rangle} f_1^q(x),$$
(12)

where M_2 is the mass of the polarized proton, $p_T \equiv |\mathbf{p}_T|$, and $\langle p_T^2 \rangle = 0.25$ $(\text{GeV}/c)^2$ is deduced by assuming a Gaussian ansatz for the $\mathbf{p}_T$ dependence of f_1 in order to reproduce the azimuthal angular dependence of the SIDIS

unpolarized cross section (Cahn effect). Flavor-dependent normalization and parameters in the x dependence are fitted to SIDIS SSA data neglecting the (small) contribution of antiquarks. The resulting parameters M_0 and N_q, a_q, b_q, with $q = u, d$, are listed in Table I. The sometimes poor resolution of the fit forced us to select only the central values in order to produce meaningful numerical simulations.

Following the steps described in Sec. III-1 of Ref. [21], in particular, the predicted sign change of $f_{1T}^\perp$ when going from SIDIS to Drell-Yan, we insert the opposite of Eq. (12) into Eq. (9) and simplify it down to

$$c_4 \approx \frac{4M_0 q_T}{q_T^2 + 4M_0^2} \frac{1}{9} \left[8N_u \frac{(a_u + b_u)^{a_u+b_u}}{a_u^{a_u} b_u^{b_u}} x_2^{a_u} (1 - x_2)^{b_u} \right.$$
$$\left. + N_d \frac{(a_d + b_d)^{a_d+b_d}}{a_d^{a_d} b_d^{b_d}} x_2^{a_d} (1 - x_2)^{b_d} \right]. \quad (13)$$

As an alternative choice, we adopt the new parametrization described in Ref. [21]. It is inspired to the one of Ref. [37], where the transverse momentum of the detected pion in the SIDIS process was assumed to come entirely from the $\boldsymbol{p}_T$ dependence of the Sivers function, and was further integrated out building the fit in terms of specific moments of the function itself. The x dependence of that approach is retained, but a different flavor-dependent normalization and an explicit $\boldsymbol{p}_T$ dependence are introduced that are bound to the shape of the recent RHIC data on $pp^\uparrow \to \pi X$ at $\sqrt{s} = 200$ GeV [26], where large persisting asymmetries are found that could be partly due to the leading-twist Sivers mechanism. The expression adopted is

$$f_{1T}^{\perp q}(x, \boldsymbol{p}_T) = N_q x(1 - x) \frac{M_2 p_0^2 p_T}{(p_T^2 + \frac{p_0^2}{4})^2} f_1^q(x, \boldsymbol{p}_T)$$
$$= N_q x(1 - x) \frac{M_2 p_0^2 p_T}{(p_T^2 + \frac{p_0^2}{4})^2}$$
$$\times \frac{1}{\pi \langle p_T^2 \rangle} e^{-p_T^2/\langle p_T^2 \rangle} f_1^q(x), \quad (14)$$

where $p_0 = 2$ GeV/c, and $N_u = -N_d = 0.7$. The sign, positive for u quarks and negative for the d ones, already takes into account the predicted sign change of $f_{1T}^\perp$ from Drell-Yan to SIDIS.

TABLE I. Parameters for the Sivers distribution from Ref. [25].

Quark up		Quark down	
N_u	0.32 ± 0.11	N_d	-1.0 ± 0.12
a_u	0.29 ± 0.35	a_d	1.16 ± 0.47
b_u	0.53 ± 3.58	b_d	3.77 ± 2.59
M_0^2	0.32 ± 0.25 (GeV/c)^2		

Again, following the steps described in Sec. III-2 of Ref. [21], we can directly insert Eq. (14) into Eq. (9) and get

$$c_4 \approx x_2(1 - x_2) \left(\frac{2p_0 q_T}{q_T^2 + p_0^2} \right)^2 \frac{8N_u + N_d}{9}. \quad (15)$$

The q_T shape is different from Eq. (13) and the peak position is shifted at larger values. This is in agreement with a similar analysis of the azimuthal asymmetry of the unpolarized Drell-Yan data (the violation of the Lam-Tung sum rule [15]). But, more specifically, it is induced by the observed $x_F - q_T$ correlation in the above-mentioned RHIC data for $pp^\uparrow \to \pi X$, when it is assumed that the SSA is entirely due to the Sivers mechanism. This suggests that the maximum asymmetry is reached in the upper valence region such that $x_F \approx x_2 \sim \langle q_T \rangle /5$ [26].

B. The Boer-Mulders effect

Contrary to the Sivers effect, the lack of data for the Boer-Mulders effect does not allow one to build reasonable parametrizations either of $h_1^{\perp q}(x, \boldsymbol{p}_T)$ or of $h_1^q(x, \boldsymbol{p}_T)$. Therefore, similarly to what was done in our previous papers [17,31], the strategy of the numerical simulation is based on making guesses for the input x and $\boldsymbol{p}_T$ dependence of the parton distributions, and on trying to determine the minimum number of events required to discriminate various SSA produced by very different input guesses. In fact, this would be equivalent to state that in this case some analytic information on the structure of these TMD parton distributions could be extracted from the SSA measurement.

Following Refs. [15,17], the $\boldsymbol{p}_T$ dependence of the parton distributions is parametrized as

$$f_1^q(x, \boldsymbol{p}_T) = \frac{\alpha_T}{\pi} e^{-\alpha_T p_T^2} f_1^q(x)$$
$$h_1^{\perp q}(x, \boldsymbol{p}_T) = \frac{M_C M_H}{\boldsymbol{p}_T^2 + M_C^2} f_1^q(x, \boldsymbol{p}_T) \quad (16)$$
$$h_1^q(x, \boldsymbol{p}_T) = \frac{\alpha_T}{\pi} e^{-\alpha_T p_T^2} h_1^q(x),$$

where $\alpha_T = 1$ GeV^{-2}, $M_C = 2.3$ GeV, and M_H is the mass of the hadron involved (i.e., M_1 or M_2). In particular, the $\boldsymbol{p}_T$ dependence of $h_1^\perp$ is fitted to the measured $\cos 2\phi$ asymmetry of the corresponding unpolarized Drell-Yan cross section, which is small for $1 \lesssim q_T \lesssim 3$ GeV/c (see, for example, Fig. 4 in Ref. [15]). Correspondingly, the $\sin(\phi + \phi_S)$ SSA will turn out to be small for the considered statistically relevant q_T range (see Sec. III B).

Inserting the expressions (16) into Eq. (11) and following the steps in Sec. IV C of Ref. [17] and in Sec. VI of Ref. [15], we get

$$
\begin{aligned}
c_4 &= -\frac{2M_C q_T}{q_T^2 + 4M_C^2} \\
&\times \frac{\sum_q e_q^2 f_1^q(x_1; \bar{q}/H_1) h_1^q(x_2; q/H_2^\uparrow) + (\bar{q} \leftrightarrow q)}{\sum_q e_q^2 f_1^q(x_1; \bar{q}/H_1) f_1^q(x_2; q/H_2) + (\bar{q} \leftrightarrow q)} \\
&\approx -\frac{2M_C q_T}{q_T^2 + 4M_C^2} \frac{f(x_1; \langle\bar{q}\rangle/H_1) h_1(x_2; \langle q\rangle/H_2^\uparrow)}{f(x_1; \langle\bar{q}\rangle/H_1) f_1(x_2; \langle q\rangle/H_2)} \\
&\equiv -\frac{2M_C q_T}{q_T^2 + 4M_C^2} \frac{h_1(x_2; \langle q\rangle/H_2^\uparrow)}{f_1(x_2; \langle q\rangle/H_2)},
\end{aligned} \tag{17}
$$

where the second step is justified by assuming that the contribution of each flavor to each parton distribution can be approximated by a corresponding average function [17].

Two choices with opposite features will be selected for the ratio $h_1(x_2; \langle q\rangle/H_2^\uparrow)/f_1(x_2; \langle q\rangle/H_2)$, namely, the ascending function $\sqrt{x_2}$ and the descending one $\sqrt{1 - x_2}$, that both respect the Soffer bound. The goal is to determine the minimum number of events (compatible with the kinematical setup and cuts) required to produce azimuthal asymmetries that can be clearly distinguished like the corresponding originating distributions. We identify this as the criterion to establish when information on the analytical structure of the involved parton distributions can be extracted from SSA data.

III. RESULTS OF THE MONTE CARLO SIMULATIONS

In this section, we present results for Monte Carlo simulations of both the Sivers and the Boer-Mulders effects in the Drell-Yan process $\pi^\pm p^\uparrow \to \mu^+ \mu^- X$ using input from the previous Secs. II A and II B, respectively. The goal is twofold. On one side, to explore the sensitivity of the simulated asymmetry to the different input parametrizations of Eqs. (12) and (14), as well as to directly verify, within the reached statistical accuracy, the predicted sign change of the Sivers function between SIDIS and Drell-Yan [20]; on the other side, to make realistic estimates of the minimum number of events required to extract as detailed information as possible on the chiral-odd distributions $h_1^\perp$ and h_1.

For the Sivers effect, we consider pion beams with energy of 100 GeV hitting a transversely polarized proton target such that $\sqrt{s} \sim 14$ GeV, i.e. the same c.m. energy available at HESR at GSI in the so-called asymmetric collider mode with antiprotons of 15 GeV and protons of 3.3 GeV [17]. For the Boer-Mulders effect, it is useful to stick to lower energies in order to keep a significant statistics (see also Sec. III B); therefore, we use pion beams of 50 GeV with $\sqrt{s} \sim 10$ GeV. The muon pair invariant mass is constrained in the range $4 < M < 9$ GeV and $1.5 < M < 2.5$ GeV, respectively, in order to explore approximately the same x range and to avoid overlaps with the

resonance regions of the $\bar{c}c$ and $\bar{b}b$ quarkonium systems. The transversely polarized proton target is obtained from a NH_3 molecule where each H nucleus is fully transversely polarized and the number of "polarized" collisions is 25% of the total number of collisions [17].

In the Monte Carlo, the events are sorted according to the cross section (4), supplemented by Eqs. (5) and (6). The asymmetry is simulated by Eq. (7). In particular, for the Sivers effect we use Eqs. (8) and (13) or (15), according to the input parametrization selected for the Sivers function. For the Boer-Mulders effect, we use Eqs. (10) and (17). The events are divided in two groups, one for positive values (U) of $\sin(\phi - \phi_{S_2})$ in Eq. (8) or of $\sin(\phi + \phi_{S_2})$ in Eq. (10), and another one for negative values (D), and taking the ratio $(U - D)/(U + D)$. Data are accumulated only in the x_2 bins of the polarized proton, i.e. they are summed over in the x_1 bins for the pion, in the transverse momentum q_T of the muon pair and in their zenithal orientation θ.

Proper cuts are applied to the q_T distribution according to the different inputs. As for the Sivers effect, the flavor-independent Lorentzian shape in the p_T dependence of Eq. (12) produces a maximum asymmetry for $q_T \sim 1$ GeV/c and a rapid decrease for larger values. Consequently, transverse momenta are selected in the range $0.5 < q_T < 2.5$ GeV/c, because for larger cutoffs the asymmetry is diluted. For the case of Eq. (14), the peak position in q_T is shifted at higher values and the cut is modified as $1 < q_T < 3$ GeV/c. In this way, the ratio between the absolute sizes of the asymmetry and the statistical errors is optimized for each choice, while the resulting $\langle q_T\rangle \sim 1.8$ GeV/c is in fair agreement with the one experimentally explored at RHIC [26]. As for the Boer-Mulders effect, we keep the latter cut $1 < q_T < 3$ GeV/c. The θ angular dependence for the Boer-Mulders effect is constrained in the range $60° < \theta < 120°$ due to Eq. (10), because outside these limits the azimuthal asymmetry is too small [17]. On the contrary, for the Sivers effect there is no need to introduce cuts because of the $(1 + \cos^2\theta)$ term in Eq. (8) [21].

We have considered different initial samples. The Sivers mechanism is explored starting from 100 000 events with the π^- beam and 25 000 with the π^+ beam, because the Monte Carlo indicates that the cross section involving π^+ is statistically disfavored by approximately the factor 1/4 [38]; in such a way, the two samples can be collected in the same time. As for the Boer-Mulders effect, the lacking of any parametrization makes it impossible to perform an isospin analysis; hence, we used 200 000 events with the π^- beam. Statistical errors for $(U - D)/(U + D)$ are obtained by making 10 independent repetitions of the simulation for each individual case, and then calculating for each x_2 bin the average asymmetry value and the variance. We checked that 10 repetitions are a reasonable threshold to have stable numbers, since the results do not change

significantly when increasing the number of repetitions beyond 6.

A. The Sivers effect

We first consider two samples, one of 100 000 Drell-Yan events for the $\pi^- p^\uparrow \to \mu^+ \mu^- X$ reaction at $\sqrt{s} \sim 14$ GeV and for muon invariant mass in the $4 < M < 9$ GeV range, and another one of 25 000 events for the $\pi^+ p^\uparrow \to \mu^+ \mu^- X$ reaction in the same kinematic conditions. Both samples can be accumulated approximately in the same time according to Eq. (13) based on the parametrization (12) of the Sivers function [25]; as already discussed, the transverse-momentum distribution is constrained in the range $0.5 < q_T < 2.5$ GeV/c. The samples are collected in x_2 bins and for each bin two groups of events are stored, one corresponding to positive values (U) of $\sin(\phi - \phi_{S_2})$ in Eq. (8), and one for negative values (D).

In Fig. 2, the asymmetry $(U - D)/(U + D)$ is shown for each bin x_2. Average asymmetries and (statistical) error bars are obtained by 10 independent repetitions of the simulation. Boundary values of x_2 beyond 0.7 are excluded because of very low statistics. The triangles indicate the results with the π^- beam obtained by Eq. (13) assuming that $f_{1T}^\perp$ changes sign from the parametrization (12) of the SIDIS data to the considered Drell-Yan [20]. For sake of comparison, the squares illustrate the opposite results that one would obtain by ignoring such prediction. Finally, the open triangles and open squares refer to the same situation,
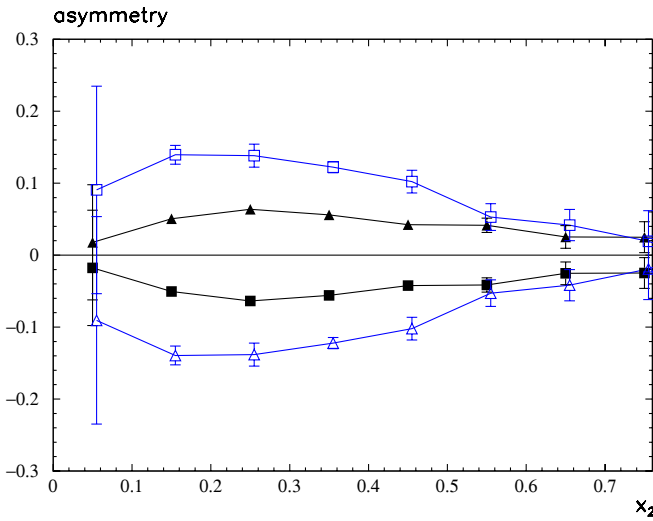
respectively, but for the π^+ beam. The sensitivity of the parameters in Table I to the HERMES results for the Sivers effect, reflects in a more important relative weight of the d quark over the u one in the valence x_2 range, with opposite signs for the corresponding normalization N_f, $f = u, d$. Consequently, in the valence picture of the $(\pi^-)\pi^+ - p$ collision where the $(\bar{u}u)\bar{d}d$ annihilation dominates, the SSA for the Drell-Yan process induced by π^+ has opposite sign with respect to π^-. Moreover, it has an absolute bigger size because the $\bar{d}d$ annihilations are weighted more than the $\bar{u}u$ ones. Apart from very low x_2 values where the parton picture leading to Eq. (1) becomes questionable, the error bars are very small and allow for a clean reconstruction of the asymmetry shape and, more importantly, for a conclusive test of the predicted sign change in $f_{1T}^\perp$.

In Fig. 3, the asymmetry $(U - D)/(U + D)$ between positive (U) and negative (D) values of $\sin(\phi - \phi_{S_2})$ in Eq. (8), is shown for each bin x_2 in the same conditions and notations as in Fig. 2, but the events are now collected according to Eq. (15) based on the parametrization (14) of the Sivers function [21], and the transverse-momentum distribution is constrained by $1 < q_T < 3$ GeV/c. The rest of the kinematics is unchanged, namely $\sqrt{s} \sim 14$ GeV and $4 < M < 9$ GeV. Notations are as in Fig. 2: the triangles indicate the results for 100 000 events with the π^- beam obtained by Eq. (15) using a positive normalization N_u, which already accounts for the sign change of $f_{1T}^\perp$ from SIDIS to Drell-Yan; the squares illustrate the results obtained by ignoring such prescription. The open triangles and open squares refer to the same situation, respectively, but for 25 000 events with the π^+ beam. Again, the opposite normalizations of the two flavors u, d, determine the opposite SSA between the π^- and the π^+ beams. But now
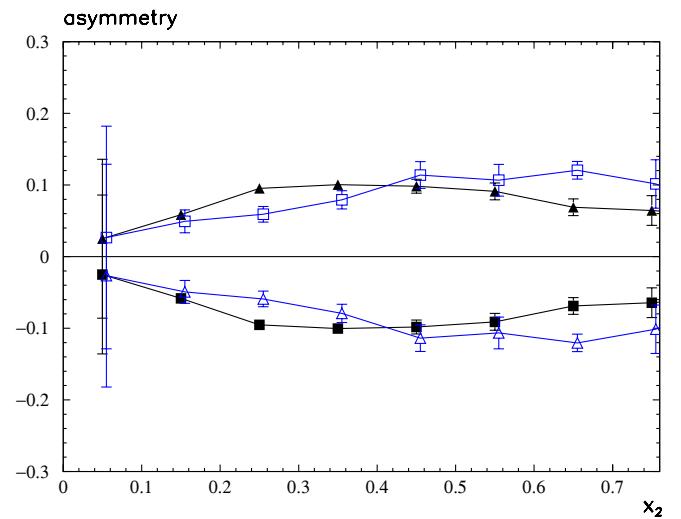

FIG. 2 (color online). The asymmetry $(U - D)/(U + D)$ with positive (U) and negative (D) values of $\sin(\phi - \phi_{S_2})$ in Eq. (8) (see text), for Drell-Yan events from the Sivers effect in the $\pi^\pm p^\uparrow \to \mu^+ \mu^- X$ reaction at $\sqrt{s} \sim 14$ GeV, $4 < M < 9$ GeV, and $0.5 < q_T < 2.5$ GeV/c, using the parametrization of Eq. (12) for the Sivers function (see text). Triangles indicate 100 000 events collected in x_2 bins for the π^- beam and with $N_u > 0$; squares for $N_u < 0$. Open triangles indicate 25 000 events for the π^+ beam and with $N_u > 0$; open squares for $N_u < 0$.

FIG. 3 (color online). The same situation with the same notations as in Fig. 2, but for the parametrization of Eq. (14) with $1 < q_T < 3$ GeV/c (see text).

in Eq. (14) the relative weight of u and d distributions is the same, hence the absolute sizes of the SSA are approximately the same irrespective of the charge of the π beam. As already anticipated in Sec. II A, the q_T distribution induced by the parametrization (14) is also related to the observed $x_F - q_T$ correlation in the RHIC data for $pp^\uparrow \to \pi X$ [26], when it is assumed that the SSA is entirely due to the Sivers mechanism. This suggests that the maximum asymmetry is reached in the upper valence region such that $x_F \approx x_2 \sim \langle q_T \rangle / 5 \sim 0.4$ for the considered cut in q_T, as it is confirmed in Fig. 3. Similarly to the case of the other parametrization, the statistical error bars are very small and allow for a detailed analysis of the (universality) properties of $f_{1T}^\perp$.

B. The Boer-Mulders effect

For the Boer-Mulders effect, we have collected 200 000 Drell-Yan events for the $\pi^- p^\uparrow \to \mu^+ \mu^- X$ reaction at $\sqrt{s} \sim 10$ GeV with muon invariant mass in the $1.5 < M < 2.5$ GeV range and $1 < q_T < 3$ GeV/c. In Fig. 4, the asymmetry $(U - D)/(U + D)$ is shown for each bin x_2 between the events with positive (U) and negative (D) values of $\sin(\phi + \phi_{S_2})$ in Eq. (10). Triangles correspond to the choice $h_1(x_2, \langle q \rangle / H_2^\uparrow)/f_1(x_2, \langle q \rangle / H_2) = \sqrt{1 - x_2}$ inside Eq. (17), open triangles to the choice $h_1(x_2, \langle q \rangle / H_2^\uparrow)/f_1(x_2, \langle q \rangle / H_2) = \sqrt{x_2}$. Here, $\langle q \rangle$ means that each term in the sum upon flavors is replaced by a common flavor-averaged contribution. Both choices re-
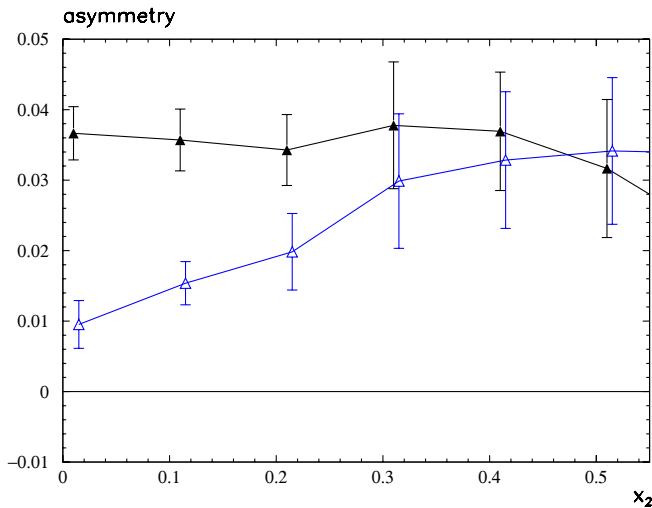

FIG. 4 (color online). The asymmetry $(U - D)/(U + D)$ with positive (U) and negative (D) values of $\sin(\phi + \phi_{S_2})$ in Eq. (10) (see text), for 200 000 Drell-Yan events from the Boer-Mulders effect in the $\pi^- p^\uparrow \to \mu^+ \mu^- X$ reaction at $\sqrt{s} \sim 10$ GeV, $1.5 < M < 2.5$ GeV, and $1 < q_T < 3$ GeV/c. Triangles for $h_1(x_2, \langle q \rangle / H_2^\uparrow)/f_1(x_2, \langle q \rangle / H_2) = \sqrt{1 - x_2}$ inside Eq. (17) (see text); open triangles for $h_1(x_2, \langle q \rangle / H_2^\uparrow)/f_1(x_2, \langle q \rangle / H_2) = \sqrt{x_2}$. Here, $\langle q \rangle$ represents a common average term that replaces each contribution in the flavor sum (for further details, see text).

spect the Soffer bound between h_1 and f_1 and have an overall normalization $2/3$, which seems a reasonable expectation on the basis of lattice results and first SIDIS experimental data [15]. The error bars are only statistical and are very small because of the copious statistics. As it is evident in the figure, for $x_2 < 0.3$ it is possible to distinguish the trend of the triangles (which statistically reflects the descending trend of the input function $\sqrt{1 - x_2}$) from the one of the open triangles (referred to the ascending $\sqrt{x_2}$). In this limited range, it should be possible to extract some information on the analytic dependence of $h_1(x)$. We made simulations also at the same kinematics of the previous Sivers effect, namely, for higher beam energy of 100 GeV and for muon pair invariant masses in the $4 < M < 9$ GeV range, but using a smaller sample of 50 000 events. The statistical error bars remain very small and the SSA is definitely nonvanishing, but a clear distinction between the two trends is no longer possible.

The overall size of the SSA is rather small and the reached statistical accuracy indicates that the size of the sample is not responsible for this feature (see also Ref. [28]). Rather, it is the outcome of a combination of several sources. First of all, the $\boldsymbol{p}_T$ dependence of $h_1^\perp$ in Eq. (16): it is fixed to reproduce the data of Ref. [32], which indicate significant SSA only for very large $\boldsymbol{p}_T$ beyond the range of interest here. Second, the target dilution factor: it is unavoidably introduced by the features of the actual target that effectively reproduces a transversely polarized proton; at COMPASS the wanted polarized events are $1/4$ of the total number of collisions on the NH_3 molecule. Finally, the Soffer bound: the various choices for the ratio $h_1(x_2, \langle q \rangle / H_2^\uparrow)/f_1(x_2, \langle q \rangle / H_2)$ are tightly limited by this constraint. Last but not least, the lack of specific flavor-dependent parametrizations for $h_1^q(x, \boldsymbol{p}_T)$ and $h_1^{\perp q}(x, \boldsymbol{p}_T)$ further reduces the selectivity power of the Monte Carlo output, as shown in Fig. 4 for $x_2 > 0.3$ and in our attempts at higher energy. This issue calls for experimental data for the $\sin(\phi + \phi_{S_2})$ asymmetry in single-polarized Drell-Yan processes, which are presently unavailable.

IV. CONCLUSIONS

In a series of previous papers [17,31], we investigated the spin structure of the proton using numerical simulations of single- and double-polarized Drell-Yan single-spin asymmetries (SSA) for the $\bar{p}^{(\uparrow)} p^\uparrow \to \mu^+ \mu^- X$ process as well as for the $pp^\uparrow \to \mu^+ \mu^- X$ one [21]. We selected muon pair invariant masses in the range $4 < M < 9$ GeV (and also $12 < M < 40$ GeV for the case of proton beams), where there is no overlap with the resonance regions of the $\bar{c}c$ and $\bar{b}b$ quarkonium systems and the elementary annihilation can be safely assumed to proceed through the $\bar{q}q \to \gamma^*$ mechanism. In particular, the Monte Carlo was based on the Drell-Yan leading-twist cross section, because

higher twists may be suppressed as M_p/M, where M_p is the proton mass.

As for single-polarized reactions, two interesting contributions generate azimuthal asymmetries of the kind $\sin(\phi + \phi_S)$ and $\sin(\phi - \phi_S)$, where ϕ and ϕ_S are the azimuthal orientations of the plane containing the final muon pair and of the proton polarization, respectively, with respect to the reaction plane. The first one involves the convolution of the transversity h_1, the missing piece necessary to complete the knowledge of the nucleon spin structure at leading twist, and the Boer-Mulders $h_1^\perp$, another chiral-odd parton density which is most likely responsible for the violation of the Lam-Tung sum rule, the long-standing problem of an anomalous $\cos2\phi$ asymmetry of the corresponding unpolarized Drell-Yan cross section [15]. The second convolution involves the so-called Sivers function $f_{1T}^\perp$ [9], a "naive T-odd" partonic density that describes how the distribution of unpolarized quarks is distorted by the transverse polarization of the parent hadron. As such, $f_{1T}^\perp$ contains unsuppressed information on the orbital motion of hidden confined partons and on their spatial distribution inside the proton [19].

In this paper, we have reconsidered the same scenario but for the $\pi^\pm p^\uparrow \to \mu^+ \mu^- X$ process at kinematics suitable for the COMPASS setup. As with antiproton beams, the elementary mechanism is dominated by the annihilation between valence partons (from p) and valence antipartons (from π). Taking advantage on the high statistics reachable with pions, in our Monte Carlo we have simulated both $\sin(\phi \pm \phi_S)$ SSA in the Drell-Yan cross section. For the Sivers effect, we selected pion beams of 100 GeV on transversely polarized fixed proton targets such that $\sqrt{s} \sim 14$ GeV, and we used two parametrizations of $f_{1T}^\perp$: the one of Ref. [25], which was deduced by fitting the recent HERMES data for the $\sin(\phi - \phi_S)$ SSA in SIDIS [2]; the one of Ref. [21], which is constrained by the recent RHIC data for the $pp^\uparrow \to \pi X$ process at higher energy [26], when it is assumed that the SSA is driven by the Sivers mechanism only. The main difference is that the former displays an emphasized relative importance of the unfavored d quark, and it gives an average transverse momentum $\langle q_T \rangle$ of the lepton pair lower than the latter. Consistently, we have built SSA by integrating the q_T distribution with adequate cuts, namely $0.5 < q_T < 2.5$ GeV/c for the former parametrization, and $1 < q_T < 3$ GeV/c for the latter one. Results have been presented as binned in the parton momenta x_2 of the polarized proton, i.e. by integrating also upon the antiparton partner momenta x_1 and the zenithal muon pair distribution θ with no further cuts. For the Boer-Mulders effect, since there is no such abundance of data and fits, similarly to Ref. [17] we have used very different input test functions and we have explored the sensitivity of the simulated $\sin(\phi + \phi_S)$ asymmetry within the reached statistical accuracy, integrating q_T in the range $1 < q_T < 3$ GeV/c. The overall size of the asymmetry is small due to constraints that are largely model independent; moreover, the predictive power of the Monte Carlo is reduced by this crude flavor-independent analysis. Hence, we have tried to counterbalance this trend by collecting a larger sample using pion beams at the lower energy of 50 GeV (hence, $\sqrt{s} \sim 10$ GeV) and at lower muon invariant masses, $1.5 < M < 2.5$ GeV. Again, results have been presented as binned in x_2 by integrating also upon x_1 and θ, but with the further constraint $60° < \theta < 120°$ induced by the factor $\sin^2\theta$ which drives the angular distribution of muon pairs.

Given the very different situations for the two analyses, also the goals are different. For the Sivers effect, the numerical simulation aims to establish the necessary statistical accuracy to distinguish different input parametrizations and to test the (universality) properties of the Sivers function, in particular, its predicted sign change when going from SIDIS to the Drell-Yan process [20]. As for the Boer-Mulders effect, the goal is to make input guesses and to try to determine the minimum number of events required to discriminate various SSA produced by very different input guesses, that would allow one to extract as detailed information as possible on the chiral-odd distributions $h_1^\perp$ and h_1.

In all cases, sorted events have been divided in two groups, corresponding to opposite azimuthal orientations of the muon pair with respect to the reaction plane (conventionally indicated with U and D), and the asymmetry $(U - D)/(U + D)$ has been considered. Statistical errors have been obtained by making 10 independent repetitions of the simulation for each individual case and, then, calculating for each x_2 bin the average asymmetry and the variance. For the Sivers effect, a starting sample of 100 000 events has been selected for the π^- beam. Since, from the Monte Carlo, the cross section with π^+ turns out statistically unfavored by a factor $1/4$ [38], we have reduced the sample to 25 000 events for the π^+ beam in order to compare situations with the same "effective luminosity." As for the Boer-Mulders effect, because of the unavailability of fits and isospin analyses, we have used 200 000 events with the π^- beam. In all cases, the $1/\tau$ behavior of the cross section, induced by the γ^* propagator, has a twofold effect. It produces the highest density of events for bins in the valence domain, typically for $x_2 \sim 0.3$. At the given $\sqrt{s}$, it also grants that the considered invariant mass range allows to explore the most populated portion of phase space, while avoiding overlaps with ranges where the elementary mechanism could be more complicated and the leading-twist analysis more questionable. The direct consequence is that, with a very large statistics of pions available, very small error bars are reached, except for boundary x_2 values.

The availability of different parametrizations of the Sivers function, obtained from independent sets of data, allows for a deep analysis of the flavor dependence of the

resulting Drell-Yan SSA, as well as for a test of the universal properties of this parton density. It turns out that the asymmetry always changes sign when switching from the π^- to the π^+ beam, because in the valence picture of the $(\pi^-)\pi^+ - p$ collision the $(\bar{u}u)\bar{d}d$ annihilation dominates, and both parametrizations considered here have weights with opposite signs for the u and d valence quarks. The parametrization of Ref. [25], being deduced by SIDIS data for the Sivers effect [2], displays a more important relative weight of the d quark over the u, which reflects in a smaller absolute size of the SSA with the π^- beam with respect to the π^+ case. No such evidence is shown by the parametrization of Ref. [21], constrained by data for the $pp^\uparrow \to \pi X$ process at $\sqrt{s} = 200$ GeV [26], where also the higher $\langle q_T \rangle$ induces a maximum of the asymmetry at higher x_2, typically $x_2 \sim 0.4$. In both of the considered cases, we have simulated the asymmetry assuming or neglecting the predicted sign change of the Sivers function when replacing the SIDIS with the Drell-Yan process [20]. The corresponding results have, of course, opposite signs, but, noticeably, the very small statistical error bars allow one to clearly distinguish between one choice or the other extreme. We conclude that with the considered sample of events it is possible to perform such an important test of nonperturbative QCD using pion beams and transversely polarized proton targets in the kinematic conditions that can be prepared at COMPASS.

For the Boer-Mulders effect, the lack of data and parametrizations of the involved parton distributions forbids a thorough analysis. The $\boldsymbol{p}_T$ dependence of $h_1^\perp$ is inherited by fitting the measured $\cos 2\phi$ asymmetry of the corresponding unpolarized Drell-Yan cross section; for the statistically relevant range $1 \lesssim q_T \lesssim 3$ GeV/c, the $\sin(\phi + \phi_S)$ asymmetry turns out to be small. We have further approximated the transversity distribution by using a ''flavor-averaged'' ratio between $h_1(x_2)$ itself and the unpolarized parton distribution $f_1(x_2)$, and we have simulated it by integrating upon x_1, q_T, θ, and inserting very different input test functions of x_2, one ascending and one descending, but all satisfying the general constraints (like the Soffer bound, that puts a strong upper bound on the size of h_1 and, consequently, of the spin asymmetry). The small statistical errors allow one to conclude that the resulting $(U - D)/(U + D)$ asymmetries, though small, are certainly nonvanishing. Two different trends in x_2 can be clearly distinguished only for $x_2 \leq 0.3$, corresponding to the ascending and descending input functions. The same conclusion is not possible at higher x_2 and, in general, at higher muon invariant masses, like for the range $4 < M < 9$ GeV adopted in the analysis of the Sivers effect. Hence, we conclude that in the present stage useful information on the transversity h_1 and/or the Boer-Mulders function $h_1^\perp$ could be extracted only for low invariant masses of the final muon pair, $1.5 < M < 2.5$ GeV, and for a limited range of parton momenta.

[1] A. Airapetian *et al.* (HERMES Collaboration), Phys. Rev. Lett. **94**, 012002 (2005).

[2] M. Diefenthaler, AIP Conf. Proc. **792**, 933 (2005).

[3] H. Avakian, P. Bosted, V. Burkert, and L. Elouadrhiri (CLAS Collaboration), in *Proceedings of the 13th International Workshop on Deep-Inelastic Scattering (DIS 05), Madison, Wisconsin, 2005* [AIP Conf. Proc. 792, 945 (2005)].

[4] V. Y. Alexakhin *et al.* (COMPASS Collaboration), Phys. Rev. Lett. **94**, 202002 (2005).

[5] M. Radici and G. van der Steenhoven, CERN Courier **44**, 51 (2004).

[6] G. Bunce *et al.*, Phys. Rev. Lett. **36**, 1113 (1976).

[7] D. L. Adams *et al.* (FNAL-E704 Collaboration), Phys. Lett. B **264**, 462 (1991).

[8] G. L. Kane, J. Pumplin, and W. Repko, Phys. Rev. Lett. **41**, 1689 (1978).

[9] D. W. Sivers, Phys. Rev. D **41**, 83 (1990).

[10] J. C. Collins, Nucl. Phys. **B396**, 161 (1993).

[11] J. Qiu and G. Sterman, Phys. Rev. Lett. **67**, 2264 (1991);

see also A. Efremov and O. Teryaev, Yad. Fiz. **39**, 1517 (1984).

[12] X.-d. Ji, J.-p. Ma, and F. Yuan, Phys. Rev. D **71**, 034005 (2005).

[13] J. C. Collins and A. Metz, Phys. Rev. Lett. **93**, 252001 (2004).

[14] D. Boer and P. J. Mulders, Phys. Rev. D **57**, 5780 (1998).

[15] D. Boer, Phys. Rev. D **60**, 014012 (1999).

[16] A. Bacchetta, U. D'Alesio, M. Diehl, and C. A. Miller, Phys. Rev. D **70**, 117504 (2004).

[17] A. Bianconi and M. Radici, Phys. Rev. D **71**, 074014 (2005).

[18] A. Bianconi and M. Radici, J. Phys. G **31**, 645 (2005).

[19] M. Burkardt and D. S. Hwang, Phys. Rev. D **69**, 074032 (2004).

[20] J. C. Collins, Phys. Lett. B **536**, 43 (2002).

[21] A. Bianconi and M. Radici, Phys. Rev. D **73**, 034018 (2006).

[22] M. Maggiora *et al.* (ASSIA Collaboration), in *Proceedings of the ASI Conference on Symmetries and Spin (Spin-*

Praha 2004), Praha, 2004 [Czech. J. Phys. 55, A75 (2005)].

[23] P. Lenisa *et al.* (PAX Collaboration), econf C0409272, 014 (2004), hep-ex/0412063.

[24] J. C. Collins *et al.*, in Proceedings of the International Workshop on Transverse Polarization Phenomena in Hard Processes (Transversity 2005), Como, Italy (hep-ph/0511272).

[25] M. Anselmino *et al.*, Phys. Rev. D **72**, 094007 (2005); **72**, 099903 (2005).

[26] S. S. Adler *et al.* (PHENIX Collaboration), Phys. Rev. Lett. **95**, 202001 (2005).

[27] A. N. Sissakian, O. Y. Shevchenko, A. P. Nagaytsev, and O. N. Ivanov, Phys. Rev. D **72**, 054027 (2005).

[28] A. Sissakian, O. Shevchenko, A. Nagaytsev, O. Denisov, and O. Ivanov, Eur. Phys. J. C **46**, 147 (2006).

[29] J. C. Collins, D. E. Soper, and G. Sterman, Nucl. Phys. **B250**, 199 (1985); see also A. Efremov and A. Radyushkin, Teor. Mat. Fiz. **44**, 157 (1980) [Theor. Math. Phys. **44**, 664 (1980)].

[30] J. C. Collins and D. E. Soper, Phys. Rev. D **16**, 2219 (1977).

[31] A. Bianconi and M. Radici, Phys. Rev. D **72**, 074013 (2005)

[32] J. S. Conway *et al.*, Phys. Rev. D **39**, 92 (1989).

[33] R. S. Towell *et al.* (FNAL E866/NuSea Collaboration), Phys. Rev. D **64**, 052002 (2001).

[34] G. Altarelli, R. K. Ellis, and G. Martinelli, Nucl. Phys. **B157**, 461 (1979).

[35] O. Martin, A. Schafer, M. Stratmann, and W. Vogelsang, Phys. Rev. D **57**, 3084 (1998).

[36] M. Anselmino *et al.*, in Proceedings of the International Workshop on Transverse Polarization Phenomena in Hard Processes (Transversity 2005), Como, Italy (hep-ph/0511017).

[37] W. Vogelsang and F. Yuan, Phys. Rev. D **72**, 054028 (2005).

[38] A. Bianconi, in Proceedings of the International Workshop on Transverse Polarization Phenomena in Hard Processes (Transversity 2005), Como, Italy (hep-ph/0511170).